Supporting information

Mesoporous TiO_2/Carbon dot heterojunction photocatalyst efficiently cleaves entire types of C-O bonds in lignin under visible light

Song Han [a], Yun Zhao [a, *], Mina Liang [a], Xiangxiong Zhai [a], Qi Zhang [a], Na Sun [a], Rong Ma [c], Guoling Li [a], Zhubing Xiao [b], Zhonghai Ni [a, *]

[a] *School of Chemical Engineering and Technology, China University of Mining and Technology, Xuzhou 221116, China*

[b] *College of Chemistry and Materials Science, Huaibei Normal University, Huaibei 235000, Anhui, China*

[c] *School of Earth Sciences and Engineering, Nanjing University, Nanjing 210023, China*

[*] Corresponding authors. E-mail addresses: zhaoyun@cumt.edu.cn (Y. Zhao), nizhonghai@cumt.edu.cn (Z, H. Ni).

SI-1. Material characterization

The crystal form and grain size of the synthesized samples were tested and analyzed using an X-ray photoelectron spectrometer (XRD, Bruker, D8 ADVANCE), with a Cu-Kα (λ=1.54056Å) cathode target. The functional group structure was determined using a Fourier transform infrared spectrometer (FT-IR, Thermo Fisher Scientific, NICOLET is5). The sample's specific surface area and pore structure can be characterized using physical adsorption measurements (BET, Autosotrb-IQ2-MP-XR). The morphological structure was determined using a field emission scanning electron microscope (SEM, TESCAN, MAIA3 LMH) and an energy spectrometer (EDS, IXRF Systems, Model 550i), and the elemental distribution was recorded. The microstructure was observed using a field emission transmission electron microscope (TEM, FEI, Tecnai G2 F20). Elemental composition analysis was performed using an x-ray photoelectron spectrometer (XPS/VB-XPS, Thermo Fisher Scientific, ESCALAB 250Xi). The optical absorption properties and band gap were evaluated using a UV-Vis diffuse reflectance spectrometer (UV-Vis DRS, Hitachi, U-3900H). The separation efficiency of photogenerated carriers was determined using a fluorescence spectrometer (PL, Hitachi, F-4600) with an excitation wavelength of 365nm. Gas chromatography mass spectrometry (GC-MS, Agilent8890/5977B) is used to detect the degradation products of lignin. Analyzing the molecular weight of lignin using gel permeation chromatography (GPC, GPC50(IS5)).

The optical properties were characterized using an electrochemical workstation equipped with a standard three-electrode cell (CHI660E, Shanghai Chenhua). The reference electrode, counter electrode, and working electrode were respectively Ag/AgCl, platinum sheet (1×1 cm^2), and photocatalyst coated on indium tin oxide (ITO, 1×2 cm^2). The electrolyte was a 0.5 mol/L Na_2SO_4 solution. The transient photocurrent response was performed at a bias voltage of 0.5 V. Electrochemical impedance spectroscopy analysis was performed at open circuit potentials ranging from 0.1 to 100000 Hz. The Mott-Schottky curve was tested at a scan potential of -1.0~0.8 V and a frequency of 1.0/1.5/2.0 kHz.

SI-2. DFT functional theory calculations

Density functional theory (DFT) is one of the most widely used tools in computational chemistry, and it is extensively applied to study the physicochemical properties and structural characteristics of molecules. In this paper, DFT calculations were carried out using Gaussian 16 software to systematically analyze the electronic structure of lignin model compounds and the transformation pathways of C-O bond cleavage [1-3]. All geometric structures were optimized at the B3LYP/6-31g(d,p) theoretical level, with all atoms fully relaxed. The corresponding frequencies of the optimized geometric structures were calculated at the same theoretical level to confirm that the optimized structures correspond to the energy minimum structures. Additionally, higher-precision single-point energy calculations were performed on the optimized structures of lignin model compounds using UM062X/def2TZVP. This paper only explores and evaluates the intermediate states, reactant states, and product states in the catalytic conversion process of lignin. There may be additional energy barriers, but these were not considered due to the imbalance in electron distribution between different states. Moreover, since the catalyst only provides holes and electrons in the reaction, this paper mainly focuses on the catalytic conversion process of lignin without a catalyst.

SI-3. Extraction of lignin

Birch lignin was extracted according to previous reported [4]. 10 g of pre-ground birch wood and 100 mL methanol containing 3 mL hydrochloric acid (37%) were added to a 100 mL flask. The mixture was refluxed for 12 h under stirring, and cooled to room temperature. Residue was removed by filtration and washed with adding small portions of methanol. The filtrate was concentrated by rotary evaporation to less than 10 mL, then poured into 200 mL of ice water and vigorously stirred to yield a deep brown solid precipitate. This lignin was collected by filtration, washed with water and dried overnight under vacuum at 60 °C. Pine lignin was extracted in the same way. Wheat stalk lignin was extracted according to previous reported [5]. 6 g wheat stalk power, 3 mmol of 1-(3-sulfobutyl) triethylammonium hydrogen sulfate and 100 mL solvent of the ethanol/water (v/v = 4/1) were added to a 250 mL stainless-steel autoclave equipped with mechanical agitation (300 rpm). After purging air with N_2 three times and pressurizing to 1.0 MPa, the reactor was heated to 200°C for 30 min. After that, the mixture was cooled to ambient temperature. Residue was removed by filtration and washed with water. Then 300 mL of water was added to the filtrate for precipitating lignin, which was eventually isolated and dried at 60°C.

SI-4. Photocatalysis experiment

The photocatalytic depolymerization process of lignin model compounds was as follows: Typically, 0.125 mmol of lignin model compound was added to 5 ml of isopropanol with 0.03 M HCl and it was dissolved by ultrasonic for 30 min. Then, it was added to a sealed reactor containing 60 mg of photocatalyst. After purging with N_2 for 30 min, the reactor was sealed tightly and placed under magnetic stirring for 30 min in the dark to achieve adsorption desorption equilibrium. The resulting mixture was irradiated with a 300 W xenon lamp (CEL-PF300-T8) and 30 w 365 nm LED for a specified time. Finally, the reaction solution was filtered using a 0.22 μm filter membrane to remove the photocatalyst, and the filtrate is analyzed by high performance gas chromatography.

The operating procedure for photocatalytic depolymerization of lignin was the same (50 mg lignin, 60 mg photocatalyst, 10 ml methanol, 365 nm LED.), as the solubility of lignin in isopropanol was limited, so the solvent was changed to methanol.

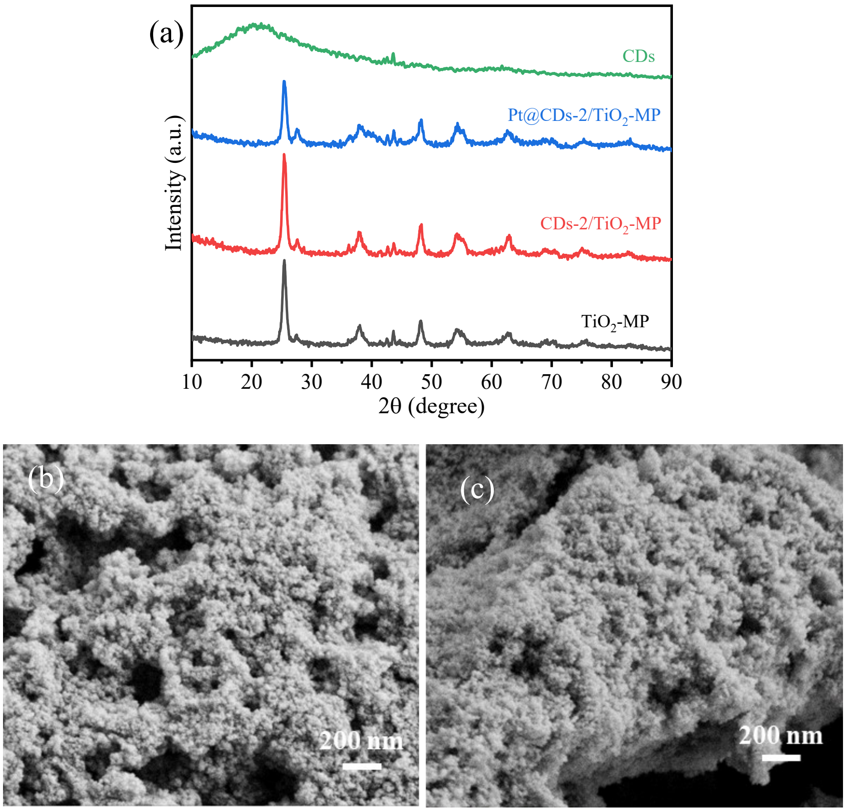

Fig. S1. (a) XRD patterns of TiO_2-MP, CDs-2/TiO_2-MP, Pt@CDs-2/TiO_2-MP and CDs, SEM image of (b) TiO_2-MP300, (c) TiO_2-MP500

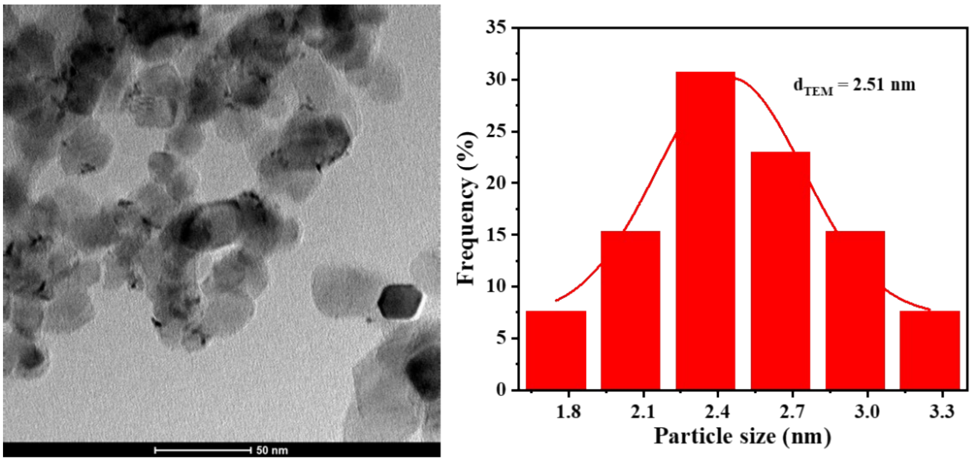

Fig. S2. TEM image of Pt@TiO_2-MP

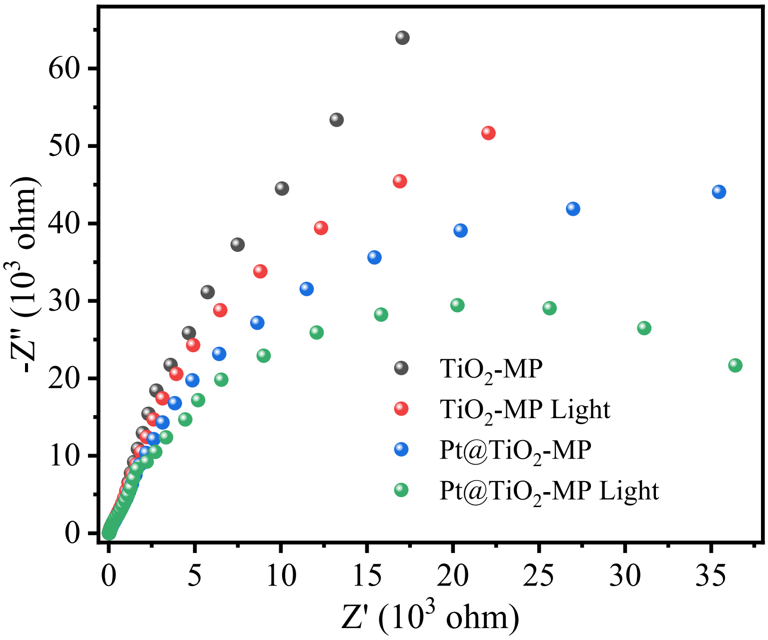

Fig. S3. EIS nyquist plots of TiO_2-MP and Pt@TiO_2-MP

Table S1. Influence of solvents on the photocatalytic reduction performance of DPE

Entry	Solvent	Conv. (%)	Yield of products (%)		
			CHE	CHL	PH
1	Isopropanol	87.8	48.3	36.1	3.4
2	Ethanol	68.3	39.2	21.0	5.9
3	Methanol	35.7	18.5	11.7	4.8
4	Acetonitrile	14.4	5.2	5.4	2.3
5	Acetone	12.0	4.0	4.0	1.7
6	Tetrahydrofuran	11.3	4.4	3.8	1.0

Reaction condition: 0.025 mmol/mL of lignin model compound, 12 mg of Pt@TiO_2-MP, N_2, 365 nm LED, HCl 0.03 M, Room temperature, 10 h

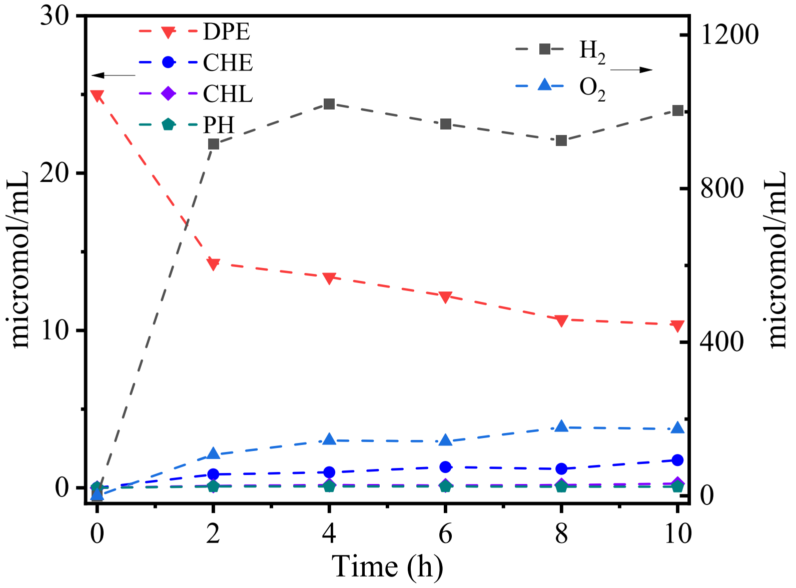

Fig. S4. Influence of aqueous solutions on the photocatalytic cracking reaction of DPE (The volume ratio of acetonitrile to water is 1:1)

Table S2. Comparison of Pt@CDs-2/TiO_2-MP catalysts with other reported catalysts for DPE hydrogenolysis

Entry	Catalyst	Reaction condition	Conv. (%)	Yield of the main products (%)				Ref.
				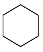	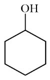	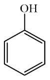	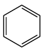	
1	Pt@CDs-2/TiO_2-MP	365 nm LED, 10 h, IPA	~100	55.9	40.2	3.4	-	This work
2	Pt@CDs-2/TiO_2-MP	Xenon lamp, 10 h, IPA	90.0	55.7	13.0	11.0	-	This work
3	Ni/ZrO_2	LED 0.5 W/cm^2, 100℃, 12 h, IPA	95.0	-	13.0	33.0	49.0	45
4	5%Pd@CN/GO/BMO(2 : 1)	150 W LED, 24 h, IPA, 5 bar H_2	74.6	34.9	-	-	-	47
5	$UO_2(NO_3)_2 \cdot 6H_2O$	Blue light, 48 h, Acetone	98.0	-	-	98.0	-	13
6	Ni/$AlP_{0.5}O_x$	150℃, 18 h, CH_3OH, 5 Mpa H_2	85.0	38	54	32	46	S6
7	5%Ru/C	120℃, 10 h, IPA	99.0	49.5	16.3	-	33.2	S7
8	Au_1Pd_1/CeO_2	180℃, 24 h, Formic acid	99.0	-	-	42.1	50.0	S8
9	Pd/HT	180℃, 5 h, IPA	27.0			27.0	27.0	S9

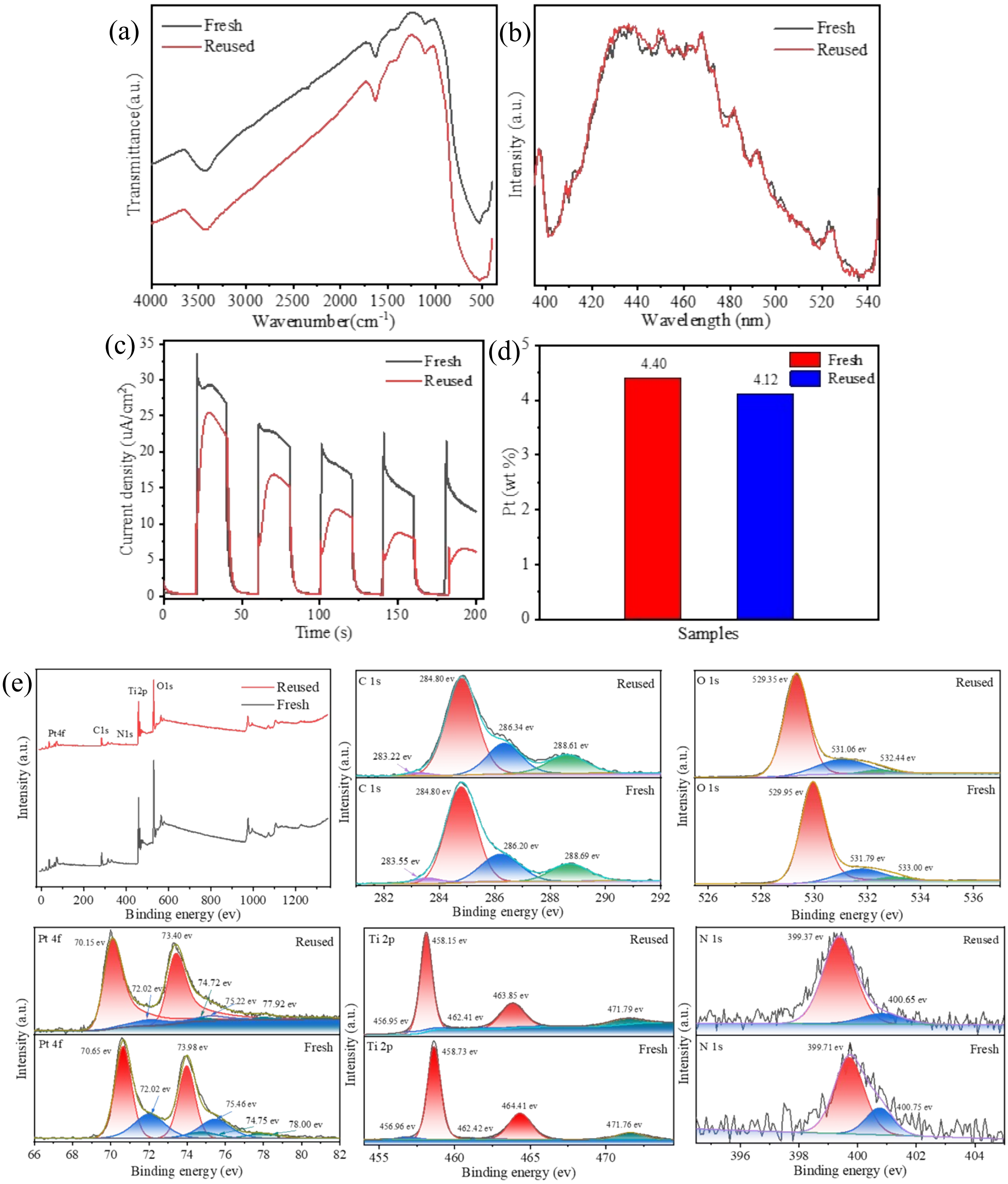

Fig. S5. (a) FT-IR, (b) PL spectrum, (c) transient photocurrent response, (d) ICP-MS and (e) XPS of fresh and reused Pt@CDs-2/TiO$_2$-MP.

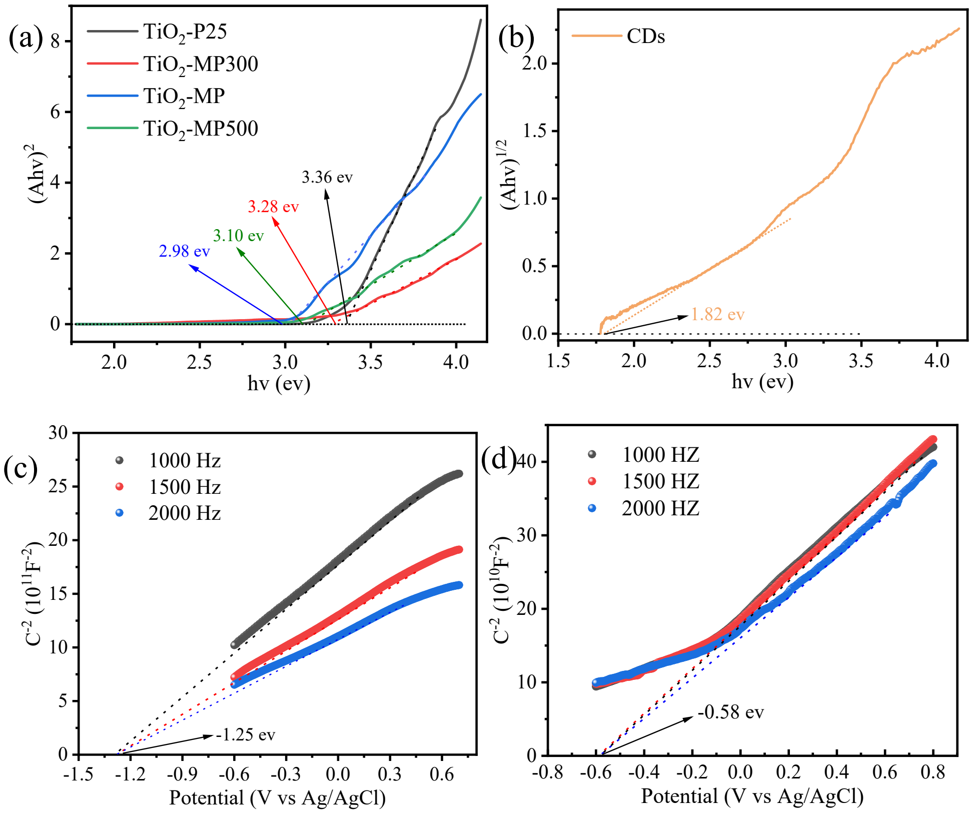

Fig. S6. Tauc plots for (a) TiO$_2$-P25, TiO$_2$-MP300, TiO$_2$-MP and TiO$_2$-MP500, (b) CDs, Mott-Schottky plots for (c) CDs and (d) TiO$_2$-MP.

Table S3. Photocatalytic reduction of DPE and its intermediates

Entry	Substrate	Conversion (%)	Yield of products (%)
1	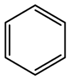	99.0	 98.2
2	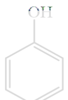	98.0	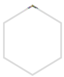 68.6  28.4
3		16.6	 14.4
4	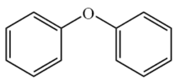	99.3	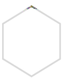 55.9 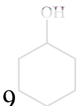 40.2 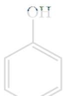 3.4
5	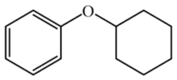	96.6	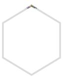 51.5 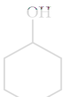 39.4 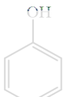 4.5
6	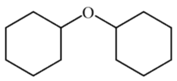	19.6	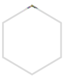 11.4  5.6

Reaction condition: 0.025 mmol/ml of lignin model compound, 12 mg of Pt@CDs-2/TiO_2-MP, 1 mL IPA, N_2, 0.03 M HCl, 365 nm LED, Room temperature, 10 h.

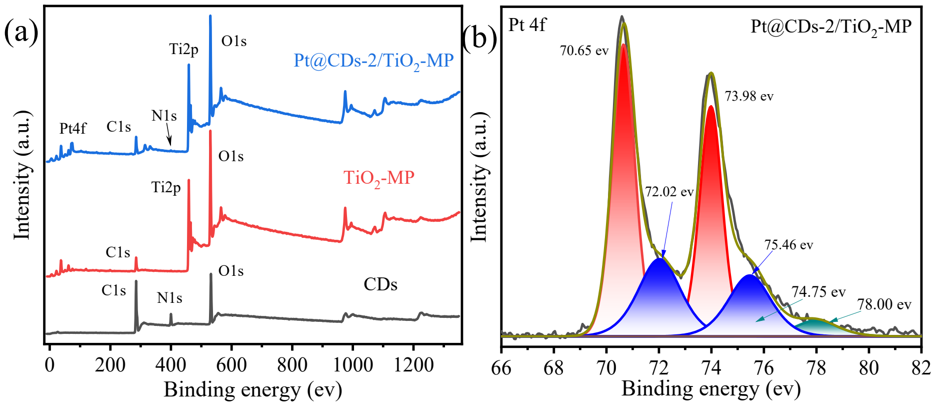

Fig. S7. (a) Survey XPS spectrum and (b) High-resolution XPS spectra of Pt.

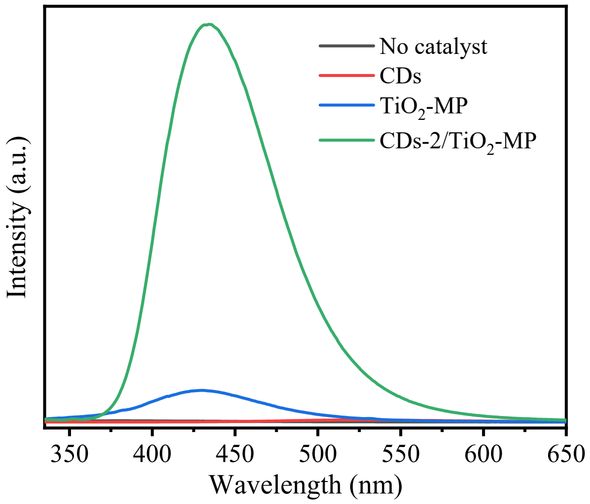

Fig. S8. Comparative fluorescence spectra of benzenepentacarboxylic acid solution after light illumination for 30 min over CDs, TiO_2-MP and CDs-2/TiO_2-MP.

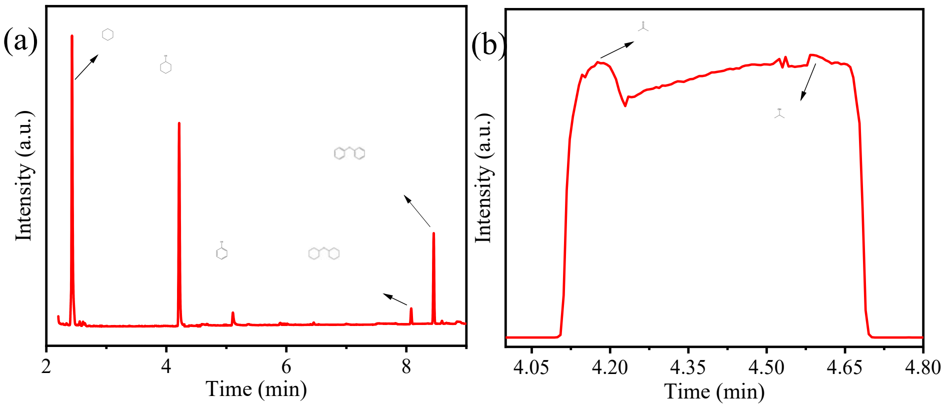

Fig. S9. (a) GC chromatograms from the photocatalytic hydrogenolysis of DPE, (b)

GC-MS related to the acetone.

Table S4. GPC analysis of dealkaline lignin, birch lignin, pine lignin and wheat straw lignin before and after photocatalytic reaction.

Entry	Sample	M_w (D_a)	M_n (D_a)	PDI (M_w/M_n)
1	Lignin (dealkaline)	714	830	1.16
2*	Lignin (dealkaline)	588	614	1.04
3	Birch lignin	783	835	1.04
4*	Birch lignin	582	625	1.07
5	Pine lignin	656	800	1.22
6*	Pine lignin	587	612	1.04
7	Wheat straw lignin	821	1083	1.32
8*	Wheat straw lignin	452	457	1.01

PDI: Polydispersity index, * Photocatalytic lignin

(a)

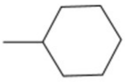
1

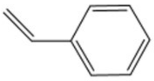
2

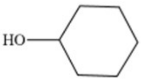
3

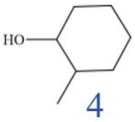
4

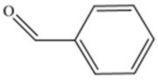
5

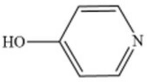
6

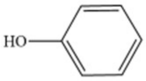
7

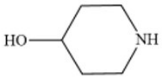
8

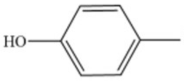
9

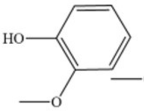
10

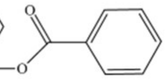
11

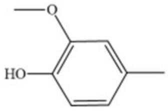
12

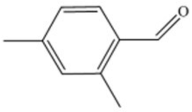
13

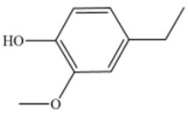
14

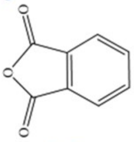
15

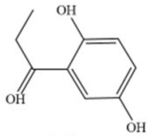
16

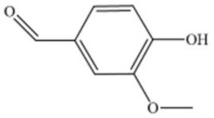
17

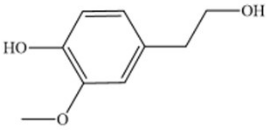
18

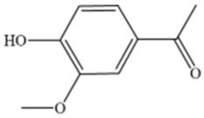
19

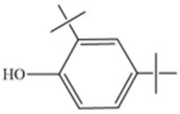
20

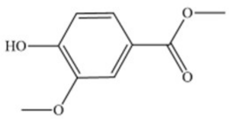
21

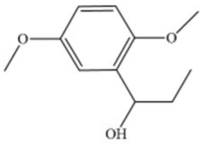
22

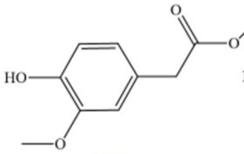
23

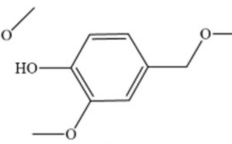
24

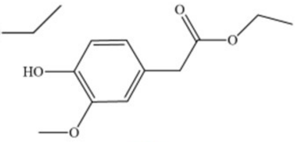
25

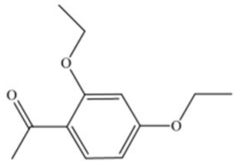
26

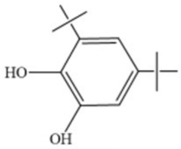
27

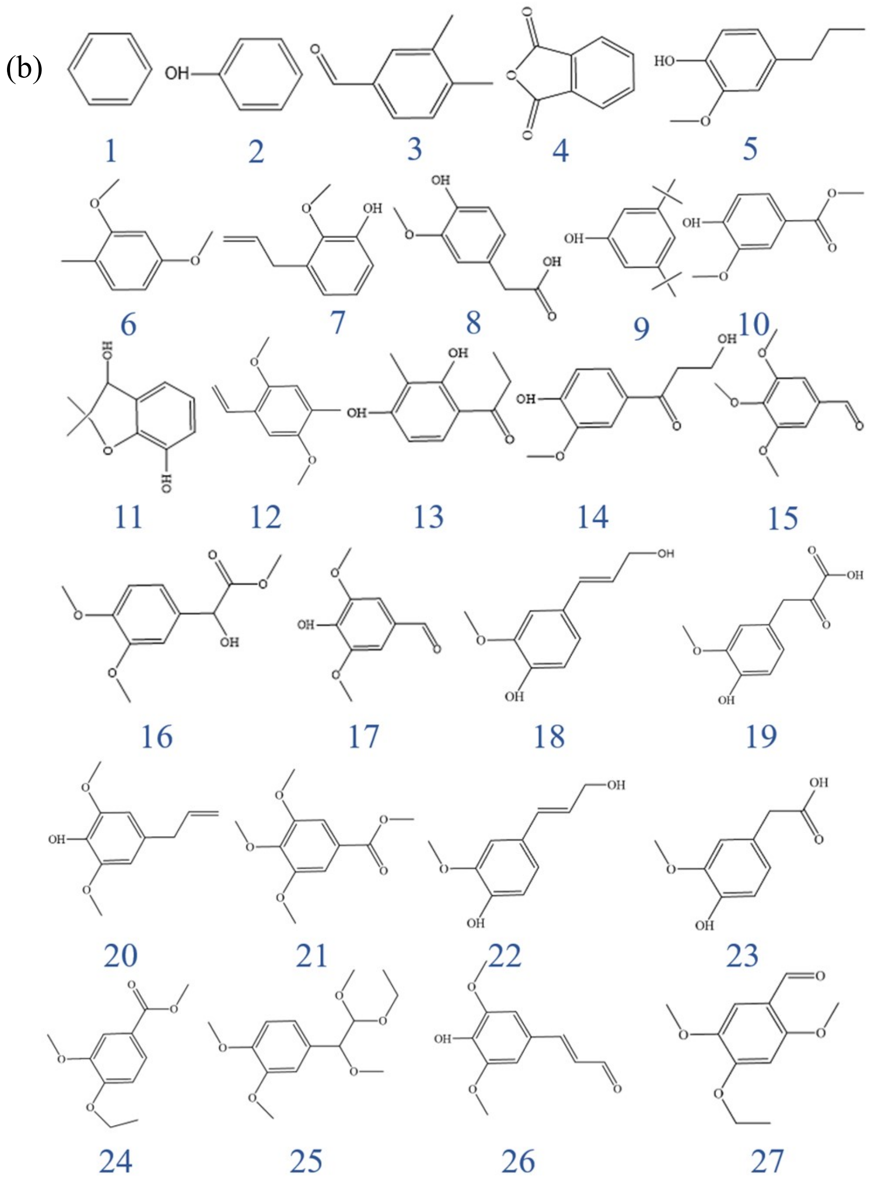
(b)
1
2
3
4
5
6
7
8
9
10
11
12
13
14
15
16
17
18
19
20
21
22
23
24
25
26
27

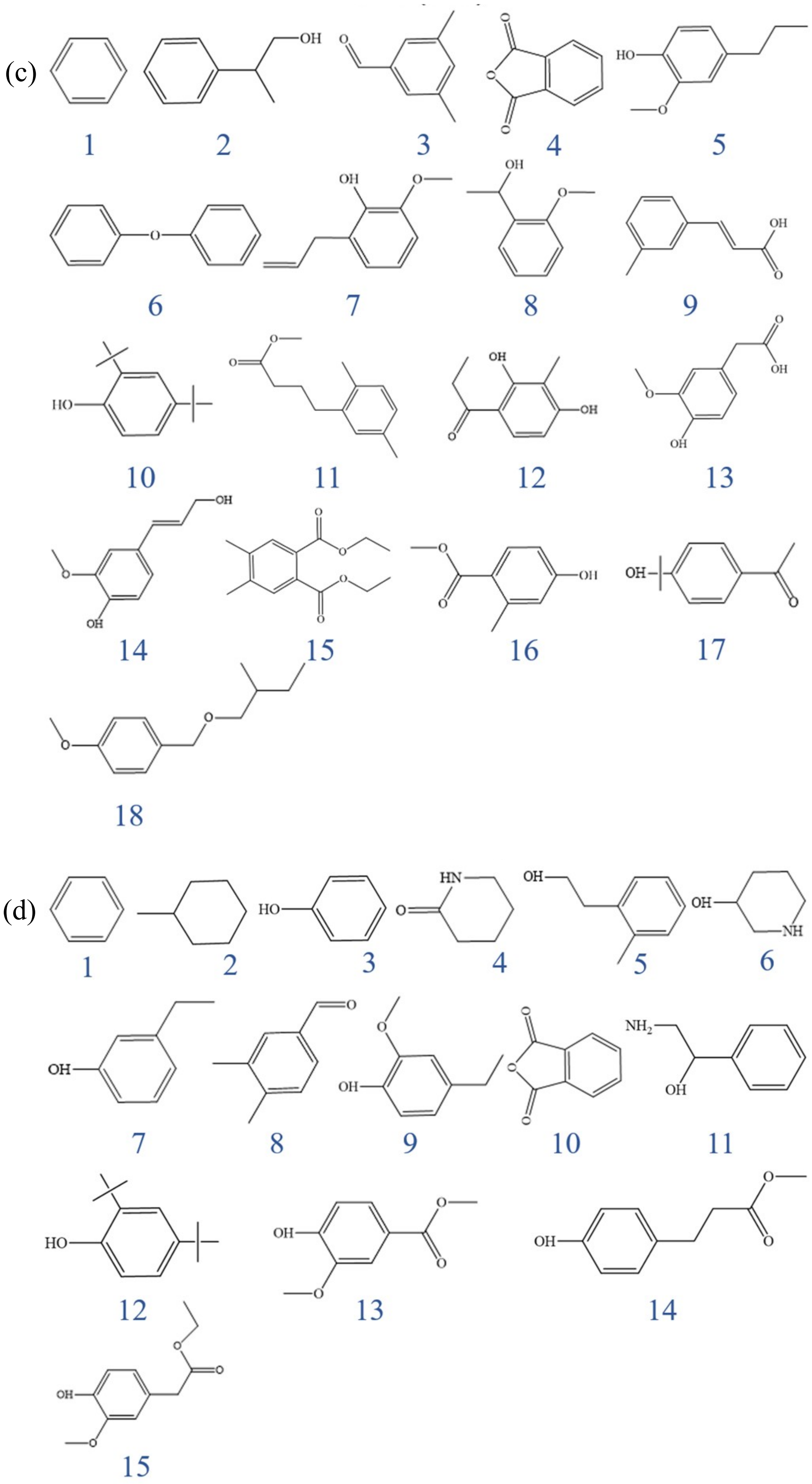

Fig. S10. GC-MS spectra of the photocatalytic conversion of (a) dealkaline lignin, (b) birch lignin, (c) pine lignin and (d) wheat straw lignin.

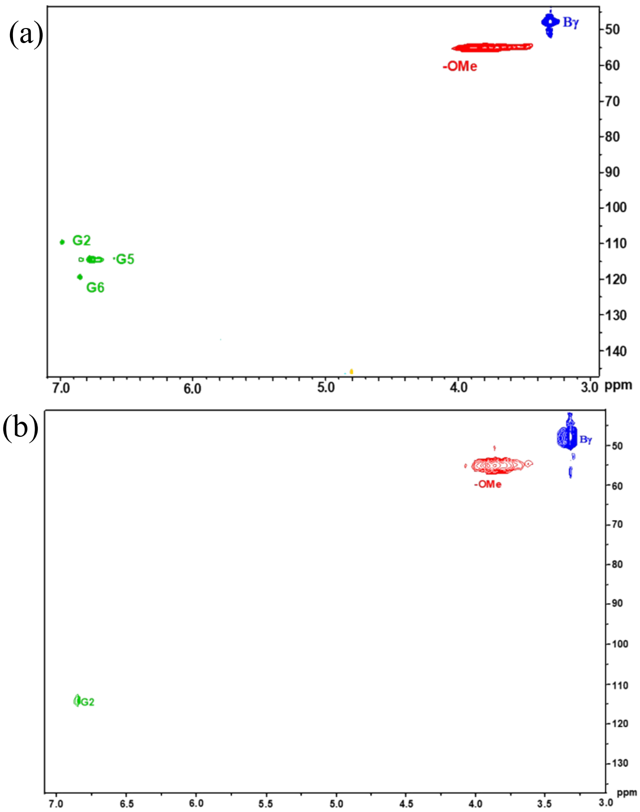

Fig. S11. 2D HSQC NMR spectra of lignin (dealkaline), (a) Before the reaction and (b) After the reaction.

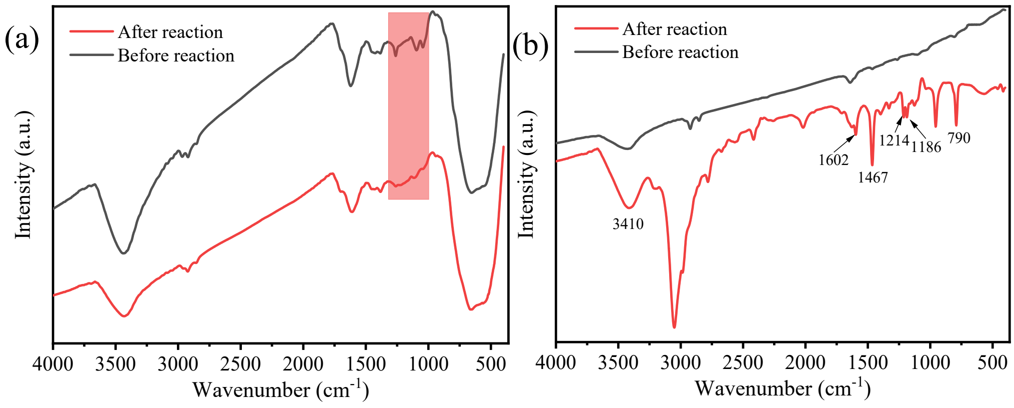

Fig. S12. The FT-IR spectra of (a) solid residue of lignite and (b) liquid product before and after photocatalytic reaction.

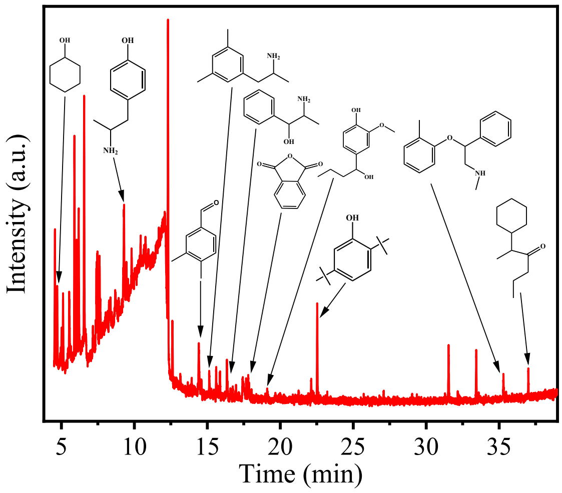

Fig. S13. GC-MS spectra of the photocatalytic conversion of Shendong lignite.

[1] H. Rao, Z. Zhu, Z. Le, Z. Xu, (2022). Qspr models for the critical temperature and pressure of cycloalkanes. *Chemical Physics Letters*. **2022**, 808, 140088.

[2] A. Shiroudi, E. Zahedi, A. R. Oliaey, M. S. Deleuze, Reaction mechanisms and kinetics of the elimination processes of 2-chloroethylsilane and derivatives: A DFT study using CTST, RRKM, and BET theories. *Chemical Physics*. **2017**, 485, 140-148.

[3] Q. Li, G. Wittreich, Y. Wang, H. Bhattacharjee, U. Gupta, D. G.Vlachos, Accurate thermochemistry of complex lignin structures via density functional theory, group additivity, and machine learning. *ACS Sustainable Chemistry & Engineering*. **2021**, 9(8), 3043-3049.

[4] Y. Shao, Q. Xia, L. Dong, X. Liu, X. Han, SF. Parker, Y. Cheng, LL. Daemen, AJ. Ramirez-Cuesta, S. Yang, Y. Wang, Selective production of arenes via direct lignin upgrading over a niobium-based catalyst. *Nat Commun*. **2017**, 8(1), 16104.

[5] D. Wang, M. Cui, Y. Li, W. Zhao, S. Ma, Z. Jiang, X. Liu, C. Liang, R. Li, L. Ma, Y. Song, Producing lignin and ethyl levulinate from wheat stalk using 1-(3-sulfobutyl) triethylammonium hydrogen sulfate and USY zeolite. *J. Agr. Food Chem*. **2023**, 71(4), 2026-37.

[6] L. Jiang, G. Xu, Y. Fu, Catalytic cleavage of the C–O bond in lignin and lignin-derived aryl ethers over Ni/AlPyOx catalysts. *ACS Catalysis*. **2022**, 12(15), 9473-9485.

[7] H. Wu, J. Song, C. Xie, C. Wu, C. Chen, B. Han, Efficient and mild transfer hydrogenolytic cleavage of aromatic ether bonds in lignin-derived compounds over Ru/C. *ACS Sustainable Chemistry & Engineering*. **2018**, 6(3), 2872-2877.

[8] X. Gao, S. Zhu, Y. Li, Selective hydrogenolysis of lignin and model compounds to monophenols over AuPd/CeO_2. *Molecular Catalysis*. **2019**, 462, 69-76.

[9] D. Dolan, R. Brucato, C. Reid, A. F. Lee, K. Wilson, A. M. Voutchkova-Kostal, Selective lignin depolymerization via transfer hydrogenolysis using Pd/hydrotalcite catalysts: model compounds to whole biomass. *Chemical Science*. **2024**, 15(48), 20223-20239.